Proceedings of the 9th U.S. National and 10th Canadian Conference on Earthquake Engineering
Compte Rendu de la 9ième Conférence Nationale Américaine et
10ième Conférence Canadienne de Génie Parasismique
July 25-29, 2010, Toronto, Ontario, Canada • Paper No 1582

PERFORMANCE LIMIT STATES OF SEISMICALLY ISOLATED BUIILDINGS WITH ELASTOMERIC BEARINGS

G. Mosqueda[1], A. Masroor[2], J. Sanchez[2] and K. Ryan[3]

ABSTRACT

The seismic performance of seismically isolated buildings under design level motions has been extensively studied, with the focus being on the nonlinear response of bearings and linear superstructure response. Base isolated buildings are typically important facilities expected to remain functional after a major earthquake. However, their behavior under extreme ground shaking is not well understood. In such an event, elastomeric bearings may become unstable under excessively large displacements or the structure may impact into the moat wall, potentially damaging the superstructure. While the stability of elastomeric bearings has been studied at the component level and few numerical studies have examined the issue of pounding in base isolated buildings, this study seeks to examine experimentally the limit states of isolated buildings systems under extreme ground motions. This paper outlines an on-going experimental program as part of the NEES Tips project which includes component testing of elastomeric bearings to characterize their stability and system level shakes table studies that will induce pounding against a moat wall, buckling of bearings and yielding of the superstructure. Results from the bearing stability tests are presented. The progress of the testing program and challenges in the shake table test, such as simulating the impact surface representative of a moat wall with soil backfill, are described.

Introduction

Past experimental and numerical studies have demonstrated the effectiveness of seismic isolation in reducing drifts and accelerations in buildings, thus reducing damage to structural and nonstructural elements. The majority of these studies have examined the response of structures under design level motions, typically linear superstructure response with nonlinear bearing behavior. While the desirable performance of seismically isolated buildings has been demonstrated for design level earthquake events, the performance of these structures under extreme ground motions is not as well understood, with only limited studies examining this issue. A potential hazard that exists when the isolation level exceeds the design displacements is that the structure can impact against the moat wall or the bearings may become unstable. Considering that seismically isolated buildings are typically critical facilities with rigorous

[1]Assitant Professor, Dept. of Civil Engineering, University at Buffalo, Buffalo, NY 14260
[2]Graduate Research Assistant, Dept. of Civil Engineering, University at Buffalo, Buffalo, NY 14260
[3]Assistant Professor, Dept. of Civil Engineering, Utah State University, Logan, UT 84321

performance requirements, it is important to better understand the superstructure response under extreme ground motions. Several numerical studies have addressed the issue of pounding against a moat wall in seismically isolated buildings (Komodromos et al. 2007), but these studies have generally relied on simplified models for impact. There is also the potential for other limit states such as buckling of elastomeric bearings or yielding of the superstructure with large ductility demands.

In order to better understand the performance limit states of seismically isolated buildings under extreme ground motions, a series of bearing component tests and shake table experiments are being conducted on ¼ scale base isolated buildings with a simulated moat wall. The superstructure is a 3 story moment resisting frame with strength and stiffness scaled from a prototype structure following similitude. The structural model will be excited under strong ground shaking to induce various performance limit states in the structure including pounding against a moat wall, buckling of elastomeric bearings and yielding of the superstructure. Individual bearing stability testing has been completed with results summarizes here. Shake table testing is planned to for late spring of 2010

Numerical Simulation of Buildings under Extreme Ground Motions

Parallel to the experimental component of this project, an analytical cost/benefit study of hypothetical code-designed conventional and base-isolated buildings is underway. For this study, theme office buildings were designed by Forell-Elsesser for a strong seismicity location in Los Angeles, California on site class D. The life cycle performance and cost of each building is being evaluated using the Performance Based Earthquake Engineering (PBEE) framework developed by PEER. As part of this study, the seismic response of the buildings has been evaluated for a range of earthquake scenarios ranging from frequent to very rare. The seismic response was determined by response history analysis of nonlinear, 3-dimensional numerical models of the building. For each scenario, 20 motions were selected and scaled according to the deaggregation of the seismic hazard. Results are available for a 3-story isolated braced frame building and moment frame building. In particular, the displacement demands of the isolators under MCE motions are of interest.

Table 1. Peak isolator displacement demands under scenario earthquakes

Scenario	Statistics	Isolator Displacements	
		Braced Frame	**Moment Frame**
72 year	Median	12.80 cm (5.04 in.)	9.53 cm (3.75 in.)
	84%	20.22 cm (7.96 in.)	16.81 cm (6.62 in.)
475 year	Median	33.53 cm (13.20 in.)	30.73 cm (12.1 in.)
	84%	64.14 cm (25.25 in.)	46.58 cm (18.34 in.)
2475 year	Median	89.28 cm (35.15 in.)	61.41 cm (24.18 in.)
	84%	148.34 cm (58.40 in.)	97.99 cm (38.58 in.)

Performance Limit States of Seismically Isolated Buildings

For these buildings, the code design displacement (ASCE 2005) D_D = 32.1 cm and the maximum displacement in the MCE is D_{TM} = 74.6 cm, which includes the effects of accidental torsion. Statistics of the observed isolator displacements for three earthquake scenarios are reported in Table 1. The median displacement of both buildings is close to the design displacement for the 475 year scenario, which suggests that the buildings achieve their target performance in the design event. However, in the 2475 year event, the 84th percentile displacement (representative of the MCE) exceeds D_{TM} by more than 25% in both buildings, and even the median displacement of the braced frame building exceeds D_{TM}. General device independent models were used for the isolation system, and did not account for limit state behavior such as pounding, buckling, or large strain hardening. These results suggest that for an isolation system designed for compliance with ASCE-7 (ASCE 2005), the displacement capacity provided by the isolation system might be exceeded in very rare motions, and the performance limit states discussed in this paper merit further evaluation. Further details of the numerical study are provided in Ryan (2010).

The numerical studies in the previous section highlight the risk of exceeding design displacements in base isolated buildings. Particularly for performance based design, it is necessary to understand and predict the behavior of buildings through collapse. This section identifies limit states of buildings isolated with elastomeric bearings and past related studies.

Stability of Elastomeric Bearings

Different types of failure mechanisms have been observed on elastomeric bearings, depending on the combination of imposed loads and deformations, material properties and boundary conditions. Some of the more common failure mechanisms include bearing instability, shear failure or tearing of the rubber, steel shim fracture and roll over in the case of bearings that are not fully anchored. In particular, bearing instability can occur at moderate displacements if the bearing load capacity is exceeded for a given displacement. Figure 1, summarizes experimental results from four previous studies on elastomeric bearing limit states. The deformation along the X-axis is normalized as shear strain while the axial load at failure is normalized by the theoretical buckling load with no horizontal deformation. This critical buckling load is defined as:

$$P_{cro} = \frac{\sqrt{G^2A_s + 4GA_sP_E} - GA_s}{2} \tag{1}$$

where,

$$P_e = \frac{\pi^2 EI_s}{h^2}, \qquad A_s = A\,\frac{h}{T_r}, \qquad I_s = I\,\frac{h}{T_r} \tag{2}$$

P_e is the Euler buckling load, G is the shear modulus and A_s is the shear area. A and I are the area and moment of inertia of the bonded rubber area, T_r is the total rubber thickness, E_r is the rotational modulus and h is the bearing height, including the rubber and the shims but excluding the end plates. For large shape factors ($S \geq 5$) EQ-1 simplifies to:

$$P_{cro} = \frac{\pi\sqrt{E_rGIA}}{T_r}, \qquad P'_{cro} = P_{cro}\left(\frac{A_r}{A}\right) \tag{3}$$

P'_{cro} is the theoretical buckling load considering lateral displacement. Figure 1 clearly demonstrate the reduction in axial load carrying capacity with lateral displacement. The bearings used in these previous studies are listed in Table 2. From Figure 1, bearings with $P/P_{cro} > 0.2$ typically failed by buckling at shears strains less than 375%. Tests with loads $P/P_{cro} < 0.2$ failed in shears at strains in the range $475\% < \delta \leq 745\%$. It is evident that at higher axial loads and small displacements bearings are susceptible to buckling while at very large displacements and small axial loads, bearings fail by shear.

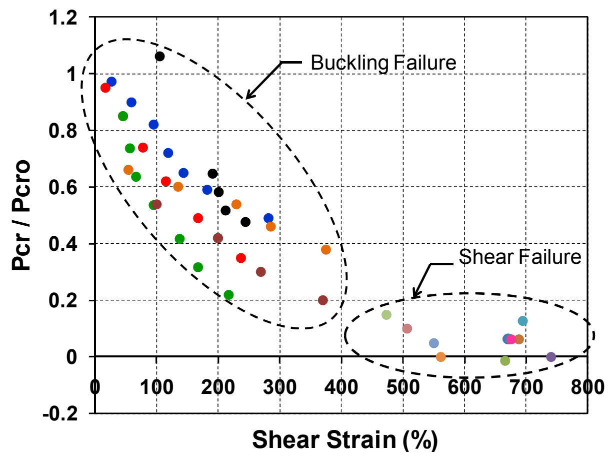

Figure1. Instability and shear failure for different types of elastomeric bearings

Table 2. Description of elastomeric bearings used in previously stability studies

Bearing	Dimensions (in)	Layers of Rubber	Thickness of Rubber (in)	Shape Factor
100 BNF	5”x5”	3	0.75”	1.67
200 BNF	5”x5”	4	0.50”	2.5
300 BNF	5”x5”	8	0.25”	5.0
500 BNF	10”x10”	4	0.50”	5.0
600 BNF	10”x10”	8	0.50”	10.0
1 – 6 CAK	Do=6.93”	20	0.87”	20.0
1 – 4 Kelly	Do=9.45”, Di=1.18”	22	0.079”	25.0
Warn	Do=5.98”, Di=1.18”	20	0.1181”	10.16

Pounding Against Moat Wall

Most structural impact studies have been analytical based on two techniques. First, the stereomechanical approach assumes impact is instantaneous and uses the principal of momentum and the coefficient of restitution (e) to modify the velocities of the colliding bodies after impact. Malhorta (2002) and DesRoches et al.(1998) used this method to investigate the behavior of bridges in seismic pounding. The second method is a force-based approach, where an axial spring with stiffness proportional to the axial stiffness of the colliding structures is used to represent the force during impact. Typical models include the Kelvin model with viscoelastic behavior (Anagnostopoulos 1988), the Hertz model with nonlinear stiffness (Davis 1992).

Few experiments have been conducted to investigate the effects of pounding. Filiatrault et al. (1995) performed a series of shaking table tests on the dynamic impact between adjacent three- and eight-story single-bay steel frames. More basic tests by Goldsmith (1960) examined collisions between spheres, spheres on plates, and other tests on bars and elastic beams.

Yielding of Superstructure

Seismically isolated buildings in the U.S. are designed to remain essentially linear during design level earthquakes. There has been some discussion as to whether the response modification coefficients (R factors) should be increased for base isolated buildings since they are relatively stringent compared to fixed-based counterparts. Numerical studies examining the yielding of superstructures in buildings (Kikuchi et al. 2007) and bridges (Constantinou, Quarshie 1998) concluded that superstructure yielding would render the isolation system ineffective, with large concentrations of deformations on the superstructure rather than the isolators. However, isolated buildings designed to current standards could still yield during extreme earthquakes. Thus, yielding of the superstructure is an important limit state that needs to be further investigated.

Experimental Stability of Elastomeric Bearings

Nine elastomeric bearings of four different types were tested to determine their stability characteristics under different loads. The bearings are listed in Table 3; Type 5 bearings have not yet been tested. A new test set up shown Figure 2 was designed for the required load and displacements capacities. The test set up is composed of two vertical actuators with a combined axial load capacity of 140 kips and one horizontal actuator with 55 kip force capacity and 12 in. stroke. Two load cells measuring shear, moment and axial load are located under the bearing. The loading system consist of two horizontal beam connected by a bracing system that only transfers horizontal forces, maintaining the actuators vertical as the bearing is deformed. The bracing system does not transfer vertical load.

The bearings were tested using two different quasi-static experimental procedures in order to compare the two methods that have been previously used to examine bearing stability. Method 1 follows a procedure previously used by Buckle et al. (1994) that applies a constant lateral displacement on the bearing then increases the axial load until the resisting shear force becomes zero. Method 2 first applies a constant axial load to the bearing followed by a horizontal displacement until the maximum shear force is achieved. Method 2 directly provides the force-displacement relationship of the bearings for constant axial loads, whereas Method 1 requires further analysis of the test data to determine stability limits. However, both of these procedures using displacement controlled bearing test machines impose constraints on the behavior of the bearings. Thus, a third method for evaluating dynamic bearing stability is proposed that provides more realistic bearing boundary conditions. A setup consisting of four bearings supporting a rigid mass will be placed on the earthquake simulator and excited to large displacements to observe the stability limits, provide more realistic conditions to assess the dynamic stability of bearings under ground shaking. These tests will serve as a benchmark to compare and validate conventional testing methods used to evaluate bearing stability limits.

Table 3. List of bearings used in stability studies

	Bearing Type 1	**Bearing Type 2**	**Bearing Type 3**	**Bearing Type 4**	**Bearing Type 5**
$Description$	Low Damping Rubber	Lead Rubber	Low Damping Rubber	Low Damping Rubber	Low Damping Rubber
Number of Bearings	2	3	2	2	2
$Shape\ Factor$	10.16	12.17	8.98	5.51	9.84
$D_o\ (in)$	5.98	5.98	6.5	5.51	9.84
$D_i\ (in)$	1.18	1.18	1.18	0.0	0.0
$A\ (in^2)$	27.0	28.1	37.4	25.9	84.0
$G_{eff}\ (ksi)$	0.1180	0.1180	0.075	0.117	0.08
$t_r\ (in)$	0.1181	0.1181	0.175	0.25	0.25
$N_r\ (\#)$	20	20	25	12	13

$D_o - bearing\ external\ diameter$
$D_i - bearing\ internal\ diameter$
$A - bearing\ area$
$G_{eff} - effective\ shear\ modulus$
$t_r - rubber\ layer\ thickness$
$N_r - number\ of\ rubber\ layers$

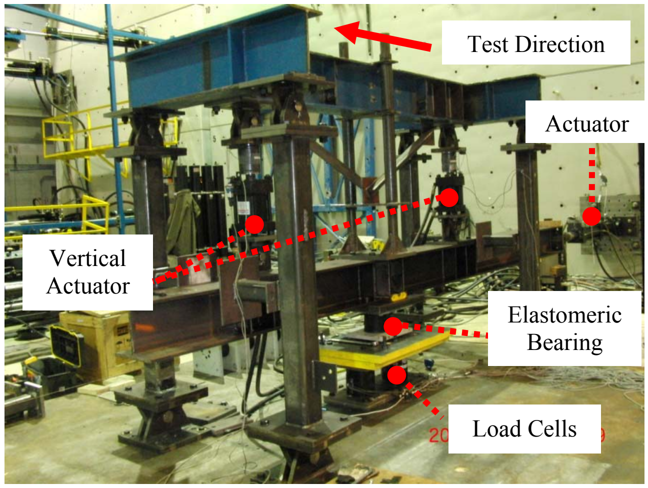

Figure 2. Experimental setup for individual bearing stability tests

Experimental Studies

The test sequence for each bearing included initial characterization tests at shear strains in the range of 25% to 200% and frequencies ranging from 0.01-1.0 Hz. Different amplitudes and frequencies were utilized in order to compare current bearings behavior with data from previous tests. The stability tests followed by applying Method 2 at various constant axial loads then Method 1 at various constant displacements. After every two stability tests, a characterization test was repeated to monitor changes in bearing behavior that could indicate damage. The range of axial loads applied during the stability tests was selected based on the bearing capacity in the undeformed configuration as an upper bound and a maximum 200% shear strain.

The results from the nine elastomeric bearings that were tested under quasi-static loading condition utilizing Method 2 are shown in Figure 3. Figures 3 (a)-(d) plot the force-displacement relation obtained from the experiment showing the dependence of the horizontal stiffness on the axial load. The data for the stability curves in Fig 3 (e)-(h) were obtained by identifying the instability point at the peak shear force with zero horizontal stiffness in Fig. 3 (a)-(d). For each of the bearing types, there is a little variation in the stability points as indicated by the small scatter in the data in Fig. 3 (e)-(f). For comparison, the theoretical stability curve obtained from Equation 3 is shown in the figures. The linear trend for the experimental results at moderate displacements is represented with the dashed line on figure 3 (e)-(f).

The stability curves and fitted trend lines for bearing Types 1 and 2 in Figures 3(e) and 4(f) show that these two bearings have similar experimental stability loads for shear strains up to 180%. These bearings are very similar, with the main difference being that Type 2 has a lead core. This data indicates that the lead plug does not contribute to the bearing critical load as would be expected by the theoretical prediction. It should also be noted that in figure 3 (f) for bearing B-11772 and B-11792, the instability points fall below the theoretical stability curve for a corresponding axial load of 80 kips. Bearings Type 3 and 4 have a smaller load capacity due to the bearings dimensions or material properties as expected (Fig 3(g) and (h)). The stability curve for these two bearings is well approximated by the theoretical formulation. This data will be further analyzed to compare both testing methods and to the upcoming shake table studies.

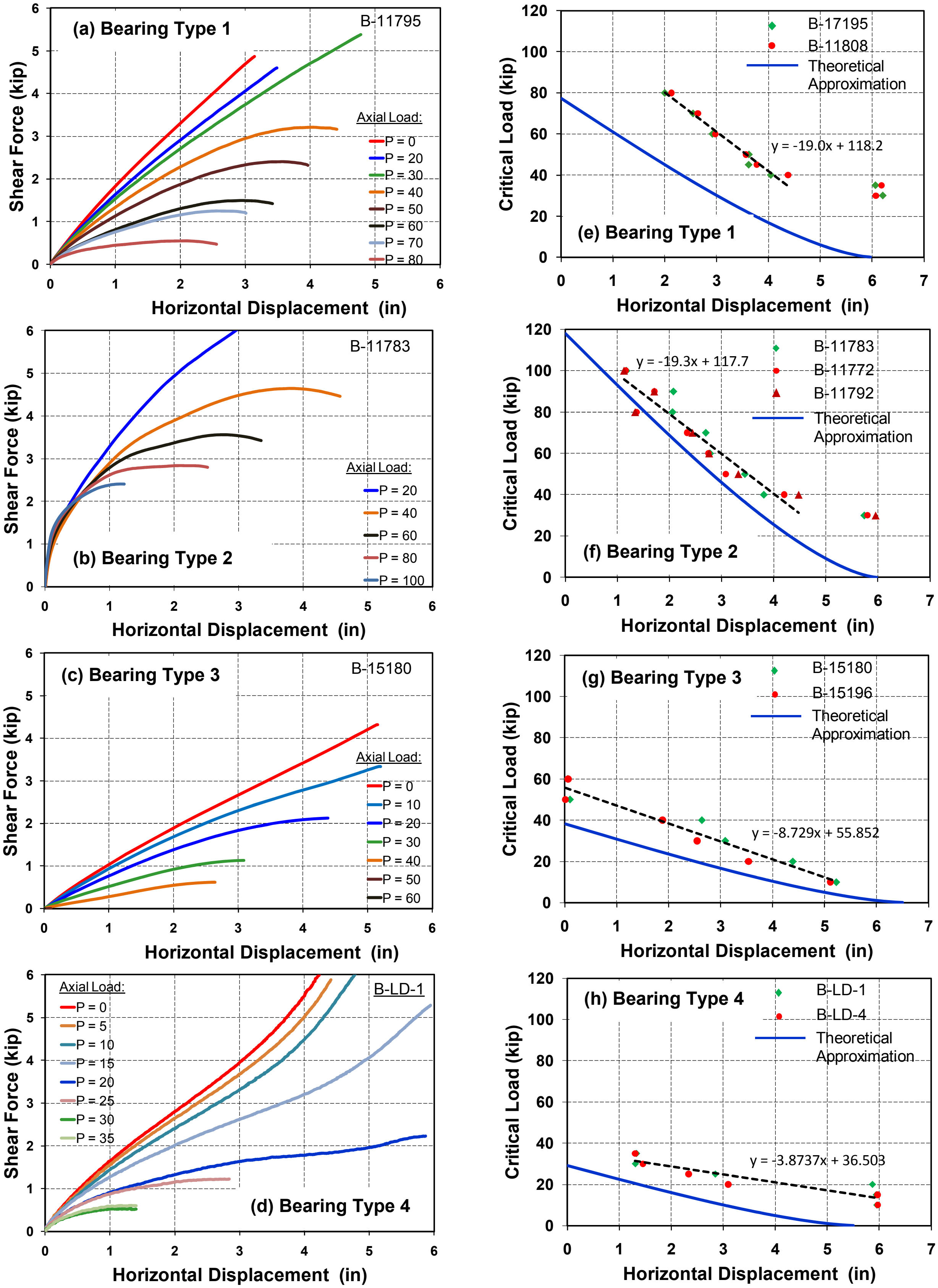

Figure 3. Left: Stability Curves for Bearing Types 1-4; Right: Shear Force vs. Horizontal Displacement Curves for the bearing listed on the figure

Earthquake Simulator Testing of Isolated Building System

Earthquake simulator studies will also be conducted on building models to examine system level behavior of buildings under extreme ground motion. The test model is extracted from a prototype frame of the case study buildings designed for the NEESTips projects. The prototype building is a rectangular three-story steel Intermediate Moment Resisting Frame (IMRF) with plan dimensions of 120 x 180 ft. The column spacing is 30 ft and the story height is 15 ft. The test specimen represents a single bay of an internal moment frame along the shorter direction of the prototype structure. The prototype frame was reduced to a quarter-scale model according to the geometric similitude law.

Unlike most previous seismic isolation tests, the limit state tests planned here have a significant potential to yield the superstructure. In order to yield the superstructure at realistic load levels, further constraints were imposed in properly scaling the strength and stiffness of the frame relative to the bearings properties. The moment frame was designed such that the scaled strength and stiffness distribution of beams and columns is comparable to the prototype. The scaled frequency of the fixed-based and isolated frame with the provided mass was also considered. The lateral resisting frame will be coupled with a gravity frame that provides the inertia for the shake table specimen; the lateral resisting frame is the only component that needs to be replaced if the superstructure is damaged. This gravity frame was developed for collapse simulations and has not been previously used on a seismically isolated building (Kusumasttuti 2005). The final scale model is a unidirectional model with a single 1 bay by 1 bay gravity frame sandwiched in between two lateral force resisting frames. The estimated superstructure weight is about 56 kips (Fig. 4). The moat model is a concrete strip with soil backfill. The moat wall model will be placed at various displacement increments in proportion to the MCE design displacements given by ASCE-7 to examine the sensitivity of this parameter and also to assess the impact at different velocities. Special attention is also given to the moat wall model.

Modeling of Moat Wall

There have been few analytical studies examining the impact of concrete slabs to retaining walls. To better assess this behavior, finite element analysis were conducted of a concrete slab representative of a building floor slab against a retaining wall with soil backfill. The objectives of these simulations were to determine the characteristics of this impact and to develop a representative scaled moat wall that could be used for the shake table studies.

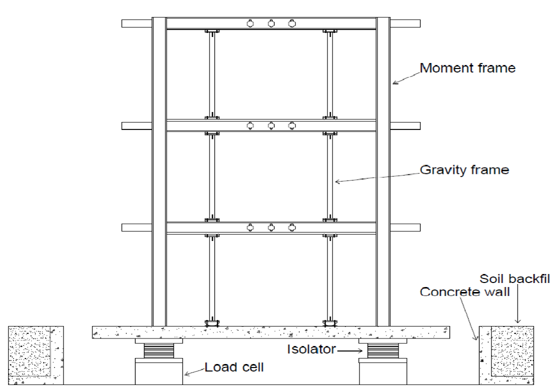

Figure 4. Earthquake simulator experimental setup of for seismically isolated building with moat wall model for performance limit state evaluation

Simulation of Moat Wall Impact

The scaled retaining wall model for impact studies consists of a concrete cantilever wall with soil backfill. In order to predict the behavior of the moat wall during the impact and identify important parameters, a series of two dimensional finite element analyses were performed in Abaqus assuming plain strain for a one mm strip. Total mass of the structure was calculated and divided by the length of the structure in the perpendicular direction of pounding and assigned to the slab. The kinematic contact method was used to model impact. The height of the wall was varied by 39, 59, 79 and 98 in and the impact velocity varied from 23.6 to 47.2 in/sec.

The results in Fig. 5 indicated that the impact force increases with velocity, but the duration of the impact does not change considerably. Also, the impact force is not sensitive to the height of the moat wall. During impact only a small portion of the wall and soil participate in pounding. Thus in order to obtain similar results from analytical solution, the only the mass corresponding to the portion of the wall that participated in the impact should be used. Although the impact force is not affected by the height of the wall, it does affect the behavior of the wall after the impact. The slab pushes the wall after the impact until either the wall collapses or the direction of the ground motion changes to separate the slab from the wall.

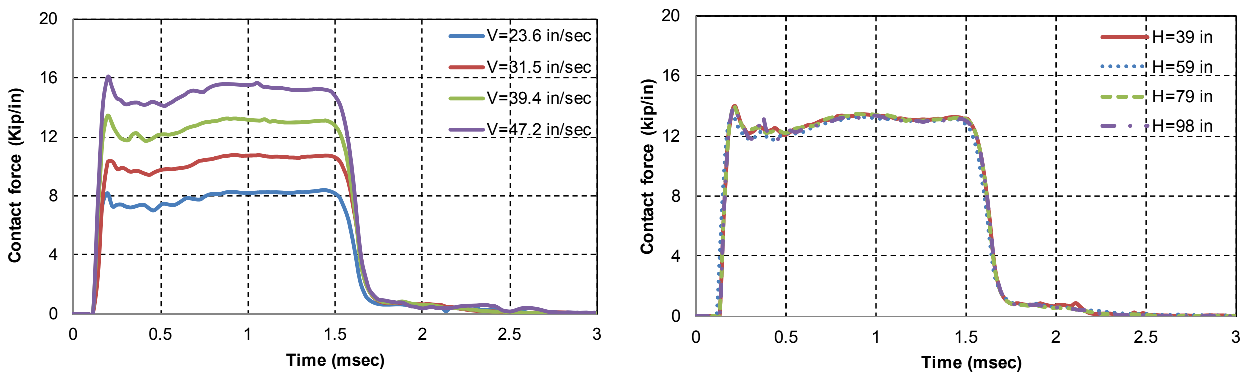

(a) (b)

Figure 5. Contact forces verses contact duration for (a) various impact velocities in 1.5 meter wall and (b) various heights of the wall for the velocity of 39.4 in/sec

Conclusions

A comprehensive experimental program is presented to evaluate the performance limit states in seismically isolated buildings. Bearing stability tests have been conducted and additional shaking table tests will examine system level behavior. Based on the bearing stability tests conducted to date, the experimental results indicate that the lead plug does not increase the buckling load in bearings as predicted by analytical approximations. Additional tests are planned to evaluate experimentally for the first time, the seismic response of isolated buildings exceeding design displacements that result in pounding against a moat wall or stability failure of bearings. The different modes of failure will be investigated to determine which is the most desirable in the case of extreme ground shaking. In order to obtain results that are representative of actual structures, a prototype building designed by practicing engineers was scaled following similitude with special attention to match the distribution of strength and stiffness between bearings, beams and columns. Further, finite element studies have been conducted to study the behavior of the moat wall during pounding to develop a representative impact barrier for the experimental setup.

Acknowledgments

This work is part of the NEESTips project supported by the National Science Foundation (NSF) under Grant No. CMMI-0724208. Any opinions, findings, conclusions or recommendations expressed in this document are those of the investigators and do not necessarily reflect the views of NSF.

References

Anagnostopoulos SA., 1988. Pounding of buildings in series during earthquakes. Earthquake Engineering and structural Dynamics. 16(3):443–456.

Buckle, I. G., and Liu, H. 1994. Experimental determination of critical loads of elastomeric isolator at high shear strain. NCEER Bulletin. 8(3), 1-5.

Buckle, I., Nagarajaiah, S., and Ferrell, K. 2002. Stability of elastomeric isolation bearings: Experimental study. *Journal of Structural Engineering,* ASCE, 128(1), 3-11.

Clark, P.W., Aiken, I.D., Kelly, J.M. 1997. Experimental Studies of the Ultimate Behavior of Seismically-Isolated Structures, *UCB/EERC-97/18*, Earthquake Engineering Research Center, University of California, Berkeley, California.

Constantinou, M.C., Whittaker, A.S., Kalpakidis, Y., Fenz, D.M., and Warn, G. 2007. Performance of Seismic Isolation Hardware under Service and Seismic Loading. Department of Civil, Structural and Environmental Engineering, University at Buffalo, State University of New York, Buffalo.

Davis RO., 1992. Pounding of buildings modelled by an impact oscillator. Earthquake Engineering and Structural Dynamics. 21(3):253–274.

DesRoches R, Muthukumar S., 2002. Effect of pounding and restrainers on seismic response of multiple-frame bridges. Journal of Structural Engineering (ASCE). 128:860–869.

Filiatrault A, Wagner P, and Cherry S., 1995. Analytical prediction of experimental building pounding. Earthquake Engineering and Structural Dynamics. 24:1131–1154.

Goldsmith W., 1960. Impact: the Theory and Physical Behaviour of Colliding Solids. Edward Arnold: London,England.

Kelly, J. (1991). Dynamic and Failure Characteristics of Bridgestone Bearings. *Report No. UCB/EERC-91-04*, Earthquake Engineering Research Center, University of California, Berkeley, California.

Kusumasttuti D. Reinhorn A.M. Rutenberg A., 2005. A versatile experimentation model for study of structures near collapse applied to seismic evaluation of irregular structures. Technical report MCEER-05-0002.

Malhotra PK., 1998. Dynamics of seismic pounding at expansion joints of concrete bridges. Journal of Engineering Mechanics (ASCE). 124:794– 802.

Minimun Design Loads for Buildings and Other Structures (ASCE/SEI 7-05), ASCE, Reston, VA, 2005.

Nagarajaiah, S., and Ferrell, K. 1999. Stability of elastomeric seismic isolation bearings. *Journal of Structural Engineering,* ASCE, 125(9), 946-954.

Ryan, K. L., Erduran, E., Sayani, P. J., and Dao, N. D., 2010. Comparative seismic response of code designed conventional and base-isolated buildings to scenario events, *Proc. 9th U.S. National/10th Canadian Conference on Earthquake Engineering,* Paper No. 1617, Toronto, Canada.